Second-order quasi-degenerate perturbation theory with *quasi*-complete active space self-consistent field reference functions

Haruyuki Nakano[a)]
Intelligent Modeling Laboratory, University of Tokyo, Tokyo 113-8656, Japan

Junji Nakatani and Kimihiko Hirao
Department of Applied Chemistry, Graduate School of Engineering, University of Tokyo, Tokyo 113-8656, Japan

(Received 5 September 2000; accepted 26 October 2000)

A quasi-degenerate perturbation theory (QDPT) is presented that is based on quasi-complete active space self-consistent field (QCAS-SCF) reference functions. The perturbation method shown here is an extension of a previously proposed QDPT with CAS-SCF reference functions (CAS-QDPT) but is a more compact perturbation method that can employ a much smaller reference configuration space with the same number of active electrons and orbitals as the CAS case. A computational scheme to second-order using a diagrammatic approach is described. The second-order effective Hamiltonian consists of the contribution from external excitations, which involve core or/and virtual orbitals, and internal excitations, which involve only active orbitals. The importance of the internal excitation contribution is emphasized. The method is tested on the potential energy curves of the LiF molecule, the Rydberg excitation energies of furan, and the transition state barrier height of the reaction, $H_2CO \rightarrow H_2+CO$. The results are in very good agreement with the corresponding CAS-SCF reference QDPT results and available experimental data. The deviations from the CAS-QDPT values in the energy are less than 0.1 eV on the average for the excitation energies of furan and less than 1 kcal for the barrier height of the reaction, $H_2CO \rightarrow H_2+CO$. The deviation from the experimental values is 0.11 eV at most for the excitation energies, and 1.2 kcal/mol, which is within the twice the experimental uncertainty, for the barrier height. © *2001 American Institute of Physics.* [DOI: 10.1063/1.1332992]

I. INTRODUCTION

Development of multireference methods represents important progress in electronic structure theory in the last two decades. In particular, multireference perturbation theories (MRPTs) based on multiconfiguration self-consistent field function references have been successfully used as efficient and accurate methods.

We have developed perturbation theory methods such as MRMP PT (multireference Møller–Plesset perturbation theory)[1–3] and MC-QDPT (quasi-degenerate perturbation theory with multiconfiguration self-consistent field reference functions).[4,5] MRMP PT is a multiconfiguration basis *single* reference state method based on Rayleigh–Schrödinger perturbation theory. MC-QDPT is a multiconfiguration basis *multi*reference state method based on van Vleck perturbation theory and therefore includes MRMP PT as a subset. Using these perturbation methods, we have clarified the electronic structures of various systems and demonstrated that they are powerful tools for investigating excitation spectra and potential energy surfaces of chemical reactions. The code of MC-QDPT[6] has been implemented in the program packages GAMESS[7] and HONDO[8] and is now open to researchers.

However, so far the implementation of these PTs is only for the complete active space self-consistent field (CAS-SCF) reference functions.[9] The CAS-SCF method and the perturbation methods based on it are certainly effective: if the active space is appropriately selected, it is applicable to any open-shell states, as well as closed-shell states, and any spin-states, and it is stable on the whole potential energy surface of chemical reactions. However, the dimension of CAS grows very rapidly as the number of active orbitals increases, which sometimes makes implementation of a perturbation computation impossible. Perturbation methods using a selected reference configuration space but retaining the advantages of the CAS-based PTs are necessary.

Recently, we proposed a quasi-complete active space (QCAS) SCF method, which is one of the multiconfiguration (MC) SCF methods and a natural extension of the CAS-SCF method.[10] In this method, the quasi-complete active space, which is a product space of CASs, is used as a variational space. The dimension of QCAS can be much smaller than the CAS that is constructed with the same number of active orbitals and electrons. We have shown that the QCAS-SCF method can yield results comparable to those of CAS-SCF, with much smaller computational cost. Combining QCAS with MC-QDPT mentioned above provides an effective tool for electronic structure theory. In this article we present MC-QDPT using QCAS-SCF reference functions. (Hereafter, we call it QCAS-QDPT, while we call MC-QDPT with CAS reference CAS-QDPT.)

Until now much effort has been devoted to developing multireference theories for an incomplete reference (or model) space.

In the 1980s, many papers were published[11–19] that

a)Electronic mail: nakano@qcl.t.u-tokyo.ac.jp

mainly treated formal aspects, such as the linked diagram expansion (LDE), in perturbation and coupled-cluster methods. These works open the possibility that more general and flexible MRPTs and MRCC (multireference coupled-cluster) methods than those based on CAS reference can play an active role. However, application of methods enjoying the benefits of the LDE for an incomplete reference space seems limited even today.

These works are for the conventional QDPT and CC method in the category of valence-universal or state-universal formalisms. MC-QDPT uses reference CI (configuration interaction) solutions that span only a subspace of the whole reference determinant or CSF (configuration state function) space as reference; hence, it is neither state-universal nor valence-universal. Thus we cannot use these results for our development of MC-QDPT based on one of the incomplete spaces, QCAS.

Two papers[20,21] were recently published on state-specific PTs with an incomplete reference space. These papers discuss practical aspects rather than formal aspects. The paper of Celani and Werner[20] proposes a second-order multireference perturbation theory for the restricted active space (RAS) and a general selected active space, which is a generalization of the second-order complete active space perturbation theory (CASPT2).[22,23] On the other hand, the paper of Grimme and Waletzke[21] presents computational strategies and algorithms for the second-order MRPT of Murphy and Messmer[24,25] with a RAS-CI wave function as reference. A selected first-order interacting space and the resolution of identity method for molecular integrals are used for further efficiency. These perturbation methods use a CI-based approach; namely the computation of the second-order energy is done via the first-order Bloch equation.

The present article is also oriented to a practical way of computing the energy of a multireference PT, MC-QDPT, at the second-order level. Here a fully diagrammatic approach is adopted. The second-order effective Hamiltonian is computed by a sum-over-orbital method without solving the first-order Bloch equation. This computation is not affected by the size of the first-order interacting space, differing from the CI-based approach. Cimiraglia[26] has proposed a diagrammatic method for CIPSI (configuration interaction by perturbation with multiconfigurational zeroth-order wave functions selected by iterative process) approach.[27] In his method, diagrams are used that are defined for the vacuum states determined so as to be identical to the reference configuration that the creation and annihilation operators act on; hence it is quite a general method. We use diagrams defined for another vacuum state, the more traditional one consisting of core orbitals. These are not so suitable for a general reference space, but are quite effective for the quasi-complete reference space.

In the QCAS-QDPT, the second-order effective Hamiltonian consists of *external* and *internal* excitation contribution, as will be shown in the next section. The external excitation is one that involves core and/or virtual orbitals in it. On the other hand, the internal excitation is an excitation among active orbitals. The internal excitation contribution plays a role that bridges the gap between QCAS-SCF and CAS-SCF. This contribution is rather small but is very important, which will be shown later by illustrative calculations.

The contents of the present article are as follows: in Sec. II, following the introduction of QCAS, formulas for the second-order QCAS-QDPT effective Hamiltonian are derived and details of the computational method are given; in Sec. III, the scheme is tested for the potential energy curves of the LiF molecule, Rydberg excitation energies of furan C_4H_4O, and the barrier height of a unimolecular dissociation reaction of formaldehyde $H_2CO \rightarrow H_2+CO$; and in Sec. IV, conclusions are drawn. Information on the diagram rule for deriving mathematical expressions from each diagram is given in the Appendix.

II. METHOD

A. Quasi-complete active space (QCAS)

In the CAS-SCF method, we partition orbitals into core, active, and virtual, then construct the CI space by distributing active electrons among the active orbitals. Let us further divide the active electron and orbital sets into N subsets and fix the number of active electrons, m_i, and orbitals, n_i, in each subset:

$$m_{\mathrm{act}}=\sum_i^N m_i, \quad n_{\mathrm{act}}=\sum_i^N n_i, \tag{1}$$

where m_{act} and n_{act} denote the number of active electrons and orbitals, respectively. We define the quasi-complete space[10,28] as the product space of CAS spanned by the determinants or CSFs as follows:

$$\mathrm{QCAS}\left[\prod_i^N (m_i,n_i)\right] = \mathrm{CAS}(m_1,n_1)\times\mathrm{CAS}(m_2,n_2)\times\cdots\mathrm{CAS}(m_N,n_N), \tag{2}$$

such that the number of electrons in each orbital group satisfies the restriction in Eq. (1).

This definition may be readily extended to the direct sum of the above QCAS [Eq. (2)],

$$\mathrm{QCAS}\left[\prod_i^M (k_i,l_i)+\prod_i^N (m_i,n_i)+\cdots\right] = \mathrm{QCAS}\left[\prod_i^M (k_i,l_i)\right]+\mathrm{QCAS}\left[\prod_i^N (m_i,n_i)\right]+\cdots, \tag{3}$$

which will appear in the application to furan in Sec. III.

B. Second-order QDPT with QCAS-SCF reference functions (QCAS-QDPT)

The effective Hamiltonian up to the second-order $K_{\mathrm{eff}}^{(0\text{-}2)}$ of van Vleck perturbation theory with unitary normalization, on which MC-QDPT[4,5] is based, is given by

$$(K_{\mathrm{eff}}^{(0\text{-}2)})_{AB}=H_{AB}+\frac{1}{2}\left\{\sum_{I\notin\mathrm{Ref}}\frac{\langle\Phi_A|V|\Phi_I\rangle\langle\Phi_I|V|\Phi_B\rangle}{E_B^{(0)}-E_I^{(0)}}+(A\leftrightarrow B)\right\}, \tag{4}$$

where $\Phi_A(\Phi_B)$ and Φ_I are reference wave functions and a function in the complement space (Q) of the reference space (P), respectively, and $E_B^{(0)}$ and $E_I^{(0)}$ are zeroth-order energies of functions Φ_B and Φ_I. The notation $(A \leftrightarrow B)$ means interchange A with B from the first term in curly brackets. Adopting (state-averaged) QCAS-SCF wave functions $\alpha(\beta)$ as reference functions $\Phi_A(\Phi_B)$ (i), which define P space, Eq. (4) becomes

$$(K_{\mathrm{eff}}^{(0\text{-}2)})_{\alpha\beta} = E_\alpha^{\mathrm{QCAS}} \delta_{\alpha\beta} + \frac{1}{2}\left\{ \sum_{I \notin \mathrm{QCAS}} \frac{\langle \alpha|V|I\rangle\langle I|V|\beta\rangle}{E_\beta^{(0)} - E_I^{(0)}} + (\alpha \leftrightarrow \beta) \right\}, \tag{5}$$

where I is now a determinant/CSF outside the QCAS. The complementary eigenfunctions of the QCAS-CI Hamiltonian (ii) and the determinants/CSFs generated by exciting electrons out of the determinants/CSFs in the QCAS (iii) are orthogonal to the reference functions and define Q space. The functions in the complementary space of P space in QCAS, namely the abovementioned (ii), however, do not appear in Eq. (5) since the interaction between the function and the reference functions is zero.

Let us define a *corresponding complete active space* (CCAS) to a QCAS as the complete active space that has the same active orbital set and electron but does not have the limitation, Eq. (1). In other words, the corresponding CAS is the minimal CAS that includes the QCAS. Then the summation for I in Eq. (2) may be divided into the summations for determinants/CSFs outside the CAS and for the determinants/CSFs outside the QCAS but inside the corresponding CAS:

$$\sum_{I \notin \mathrm{QCAS}} = \sum_{I \notin \mathrm{CCAS}} + \sum_{I \in \mathrm{CCAS} \wedge I \notin \mathrm{QCAS}}, \tag{6}$$

and then the former second-order term in Eq. (5) may be written as

$$(K_{\mathrm{eff}}^{(2)})_{\alpha\beta} = \sum_{I \notin \mathrm{CCAS}} \frac{\langle \alpha|V|I\rangle\langle I|V|\beta\rangle}{E_\beta^{(0)} - E_I^{(0)}} + \sum_{I \in \mathrm{CCAS} \wedge I \notin \mathrm{QCAS}} \frac{\langle \alpha|V|I\rangle\langle I|V|\beta\rangle}{E_\beta^{(0)} - E_I^{(0)}}. \tag{7}$$

The former term in Eq. (7) involves excitations from core orbitals and excitations to virtual orbitals in the intermediate states I, while the latter term involves excitations where only active orbitals are involved. Hereafter, we call the former term the *external* terms and the latter the *internal* terms.

The external terms may be calculated in a similar manner to the MC-QDPT with CAS reference functions (CAS-QDPT). If we adopted the particle-hole formalism using the vacuum state defined by the determinant with all the core orbitals occupied and the remaining active and virtual orbitals unoccupied, the second-order effective Hamiltonian is expressed by 25 Goldstone diagrams. These diagrams themselves are identical to those used in the open-shell or conventional quasidegenerate perturbation theory. (They are not listed here. See Ref. 29, p. 298, for example.) The difference is in the energy denominator and the coupling coefficient in deriving explicit formulas from the diagrams (see the Appendix). Take the following three-body diagram as an example:

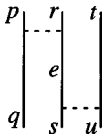

This diagram is translated to a mathematical expression according to the diagram rule in the Appendix,

$$(D_{\mathrm{ext}}^{\text{3-body}})_{\alpha\beta} = \sum_{pqrstu}^{\mathrm{act}} \sum_{e}^{\mathrm{vir}} \sum_{B}^{\mathrm{QCAS}} \frac{(pq|re)(es|tu)}{\epsilon_s - \epsilon_e + \epsilon_u - \epsilon_t - E_B^{(0)} + E_\beta^{(0)}} \times \langle \alpha|E_{pq,rs,tu}|B\rangle C_B(\beta). \tag{8}$$

In Eq. (8), $(pq|rs)$ are the two-electron integrals in the molecular orbital basis; ϵ_p are orbital energies; B is a determinant or CSF in QCAS; $C_B(\beta)$ is the QCAS-SCF CI coefficient for B in state β; $E_B^{(0)}$ is the zeroth-order energy of B; and $E_{pq,rs,tu}$ is a shift operator,

$$E_{pq,rs,tu} = \sum_{\sigma=\alpha,\beta} \sum_{\sigma'=\alpha,\beta} \sum_{\sigma''=\alpha,\beta} a_{p\sigma}^+ a_{r\sigma'}^+ a_{t\sigma''}^+ a_{u\sigma''} a_{s\sigma'} \alpha_{q\sigma}. \tag{9}$$

The definition of the orbital energies ϵ_p will be given in the subsequent subsection. The other terms are derived similarly, which are apparently the same as the ones of CAS-QDPT.

Note the following points on the computational aspects:

(1) In spite of the outward similarity, the efficiency is different. In CAS-QDPT the label B runs over the CAS while in QCAS-QDPT it runs over only the QCAS, a subspace of the CAS; hence the number of coupling coefficients between a state α and a determinant/CSF B is much smaller in QCAS-QDPT than in CAS-QDPT. Since the computational cost is roughly proportional to the number of coupling coefficients, the evaluation of the external terms of QCAS-QDPT is more efficient than that of CAS-QDPT.

(2) In a calculation of QCAS-SCF, only one- and two-body coupling coefficients appear in the computation and they are decoupled into the alpha- and beta-strings in each active orbital subset, which makes the computation of the CI part efficient.[10] On the contrary, the three-body coupling coefficients that appear in the perturbation calculation may not be decoupled in a similar manner. However, from the nature of QCAS, the three-body as well as one- and two-body coupling coefficients may be decoupled into alpha- and beta-strings. This is enough for the efficiency of the perturbation calculations, since the summation of the integral product divided by energy denominator for each coupling coefficient is the major part in computational time rather than the coupling coefficient computation.

For the calculation of the internal terms, there are several strategies. One approach is a diagram method similar to the external terms. For the internal terms only the particle lines are concerned. Hence, the 5 diagrams that do not include hole lines among the external 25 diagrams appear:

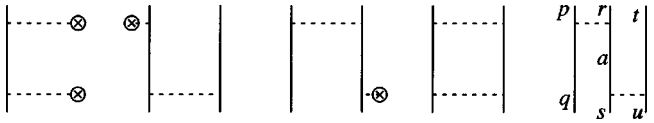

The mathematical expression for the three-body diagram is, for example, given by the following:

$$(D_{\mathrm{int}}^{\text{3-body}})_{\alpha\beta}=\sum_{pqrstu}^{\mathrm{act}}\sum_{a}^{\mathrm{act}}\sum_{B}^{\mathrm{QCAS}}\frac{(pq|ra)(as|tu)}{\epsilon_s-\epsilon_a+\epsilon_u-\epsilon_t-E_B^{(0)}+E_\beta^{(0)}}\times\langle\alpha|E_{pq,rs,tu}|B\rangle C_B(\beta). \quad (10)$$

The summations only run over active orbitals, but these summations are restricted so that the intermediate determinants/CSFs are outside the QCAS. This may be easily handled because of the nature of the QCAS. In the QCAS reference case, this restriction is done only with orbital indices without referring to the reference determinants/CSFs, whereas in the general reference case the restriction scheme also depends on the reference determinant/CSF *B*. For the internal terms, besides the connected diagrams drawn above, all the four disconnected diagrams appear that originate from the product of the one- and two-body perturbation operators:

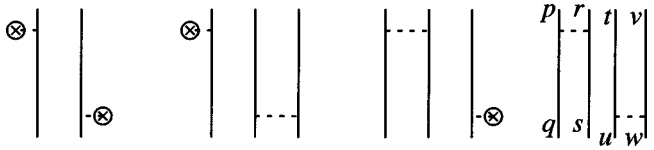

Up to four-body diagrams are necessary. The four-body term is, for example, given by

$$(D_{\mathrm{int}}^{\text{4-body}})_{\alpha\beta}=\frac{1}{4}\sum_{pqrstuvw}^{\mathrm{act}}\sum_{B}^{\mathrm{QCAS}}\frac{(pq|rs)(tu|vw)}{\epsilon_u-\epsilon_t+\epsilon_w-\epsilon_v-E_B^{(0)}+E_\beta^{(0)}}\times\langle\alpha|E_{pq,rs,tu,vw}|B\rangle C_B(\beta). \quad (11)$$

Again the summations are restricted so that the intermediate determinants/CSFs are outside the QCAS and they may be easily handled due to the nature of the QCAS for the same reason.

Another scheme is a more straightforward one where the creation and annihilation operators are not arranged in normal order and, instead, the coupling coefficients for the product of the operators are used directly. The diagrams are the same as the disconnected diagrams drawn above. However, the rule in the Appendix is somewhat different: the creation and annihilation operator part is replaced by the original product,

$$(D_{\mathrm{int}}^{\text{4-body}})_{\alpha\beta}=\frac{1}{4}\sum_{pqrstuvw}^{\mathrm{act}}\sum_{B}^{\mathrm{QCAS}}\frac{(pq|rs)(tu|vw)}{\epsilon_u-\epsilon_t+\epsilon_w-\epsilon_v-E_B^{(0)}+E_\beta^{(0)}}\times\langle\alpha|E_{pq,rs}E_{tu,vw}|B\rangle C_B(\beta). \quad (12)$$

As with the internal terms, this scheme is also effective in addition to the previous one. However, since in general the coupling coefficient for the normal ordered product $\langle\alpha|E_{pq,\cdots,rs}|B\rangle$ is sparser than that for the general product $\langle\alpha|E_{pq,\ldots}E_{rs,\ldots}|B\rangle$, this scheme is less efficient than the previous one. An advantage of this scheme is that it is readily extended to the general reference space case.

A third scheme is one where matrix operations for the Hamiltonian matrix are used:

$$(K_{\mathrm{int}}^{(2)})_{\alpha\beta}=\sum_{AB,I}C_A(\alpha)H_{AI}H_{IB}C_B(\beta)/(E_\beta^{(0)}-E_I^{(0)}). \quad (13)$$

The intermediate determinants/CSFs *I* are made by exciting one or two electron(s) from the reference QCAS determinants/CSFs within the active orbital space. In general, the number of *I* is not large, and thus they may be managed in computer memory. This scheme is especially useful when determinant/CSF selection is done. We may efficiently take into account the contribution from the unselected determinants/CSFs using Eq. (13).

In the current implementation the first scheme has been adopted. The computation is done with the coupling coefficient driven method. These coupling coefficients are sparse and can be pre-screened according to the condition,

$$(v_B^{pq\cdots rs})_{\alpha\beta}=\langle\alpha|E_{pq,\cdots,rs}|B\rangle C_B(\beta)=\sum_{A}^{\mathrm{QCAS}}C_A(\alpha)\langle A|E_{pq,\cdots,rs}|B\rangle C_B(\beta)>\delta, \quad (14)$$

where $\delta=1\times10^{-8}$ is usually sufficient to keep the energy accuracy better than 10^{-5} hartree. Thus the multiple summation for active orbitals in Eqs. (10), (11), (12), and other terms, which seemingly scales as the power of the number of active orbitals, is actually diminished considerably.

It is worth noting that the contribution of the internal terms is usually small but is very important. It plays a role that bridges the gap between QCAS-SCF and CAS-SCF. Without internal contribution, if the results include some error at QCAS-SCF levels compared to those of CAS-SCF, they cannot be recovered even if we go beyond the second-order of perturbation.

C. Definition of orbital energies

There is an arbitrariness in choosing orbitals since the QCAS-SCF energies are invariant under rotation in core and virtual orbital spaces and in *each active orbital subspace*. We determine the orbitals so that the generalized Fock matrix,

$$F_{pq}=h_{pq}+\sum_{rs}D_{rs}^{\mathrm{Ave}}\left[(pq|rs)-\frac{1}{2}(ps|rq)\right], \quad (15)$$

is diagonal in each orbital space and sub-space, where D_{rs}^{Ave} represents the averaged one-particle density matrix, and define their energies ϵ_p by the corresponding diagonal elements F_{pp}. This definition is simply an extension from the CAS-QDPT case.

III. APPLICATIONS

We applied the present method to some molecular systems to illustrate its performance. We calculated with QCAS-QDPT the potential energy curves (PECs) of the two lowest $^1\Sigma^+$ states of the LiF molecule, Rydberg excited states of furan C_4H_4O, and the transition state barrier height of the reaction $H_2CO\rightarrow H_2+CO$, and compared the results with those of CAS-QDPT with corresponding active spaces.

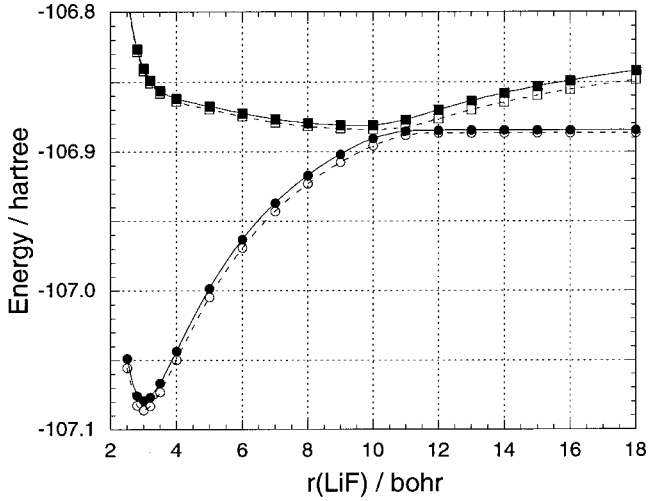

FIG. 1. The QCAS-SCF (●,■) and CAS-SCF (○,□) potential energy curves of the two lowest $^1\Sigma^+$ states of LiF.

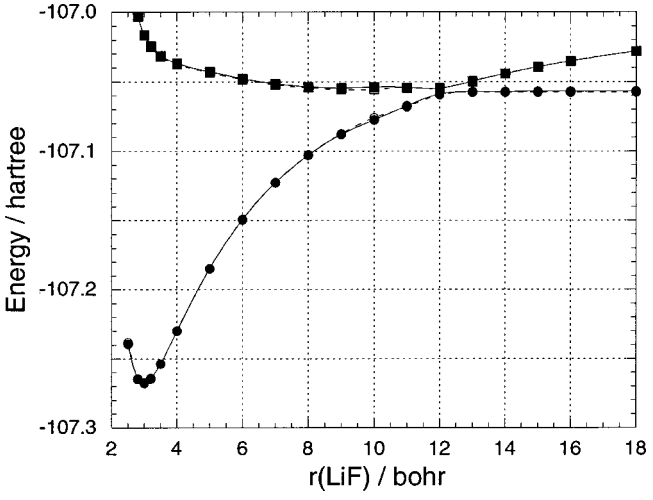

FIG. 2. The QCAS-QDPT (●,■) and CAS-QDPT (○,□) potential energy curves of the two lowest $^1\Sigma^+$ states of LiF.

A. Potential energy curves of the two lowest $^1\Sigma^+$ states of the LiF molecule

The first example is the calculation of the PECs of the two lowest $^1\Sigma^+$ states of the LiF molecule. In the diabatic picture, one of the $^1\Sigma^+$ states is ionic and the other state is covalent. In the equilibrium structure region the ionic state is lower in energy (the ground state), while at the dissociation limit the covalent state is lower. The two potential curves therefore show avoided-crossing in the middle in the adiabatic picture. It has been reported[4,30] that these two adiabatic states strongly interact in the avoided-crossing region and single-state multiconfigurational perturbation theories failed in that region.

The basis set used is 6-311++G($3df$,$3pd$).[31] The active spaces were constructed from six electrons and nine (4σ-6σ, 1π-3π, and $1\pi'$-$3\pi'$) orbitals. CAS was used for comparison and was constructed by distributing these six electrons among all nine orbitals. QCAS was constructed by first dividing the orbitals into three groups, $\{4\sigma$-$6\sigma\}$, $\{1\pi$-$3\pi\}$, and $\{1\pi'$-$3\pi'\}$, and then distributing two electrons among each group. Hereafter, we call this active space QCAS$[(2,3)^3]$. The dimension of this QCAS is 729 (in Slater determinants basis; without symmetry) and that of the corresponding CAS is 7 056. The 1σ orbital corresponding to F($1s$) was frozen in the perturbation calculations.

Results are shown in Figs. 1–3. Figure 1 shows PECs at the QCAS- and CAS-SCF levels and Fig. 2 shows PECs at the QCAS- and CAS-QDPT levels. The errors of the reference function (QCAS-SCF/CAS-SCF) level and perturbation theory (QCAS-QDPT/CAS-QDPT) level are plotted in Fig. 3. The QCAS-SCF curves have systematic errors from the CAS-SCF results depending on the nature of the states: about 4 kcal/mol for the ionic state (in the diabatic picture; lower the near equilibrium structure, higher at the dissociation limit) and about 1.5 kcal/mol for the covalent state. These are well recovered by QCAS-QDPT. At this level, the errors from CAS-QDPT are less than 1 kcal/mol for both states, except for one point ($r=10.0$ bohr).

Plotted in Fig. 4 is the energy difference between QCAS-QDPT results without the internal term contribution (i.e., external only term contribution) and CAS-QDPT results as well as that between QCAS-SCF and CAS-SCF results. This figure well illustrates the importance of the contribution from the internal terms. The external term only contribution describes PECs relatively well and the errors are small to be sure, but the error pattern is similar to that of the QCAS-SCF against CAS-SCF. This indicates that, when the PECs have a deficiency at the QCAS-SCF level, without the internal term contribution this deficiency is carried over to the QCAS-QDPT level. The internal terms are essential for balanced description of relative energies or potential energy surfaces although the contribution is small and sometimes the four-body internal terms are time-consuming.

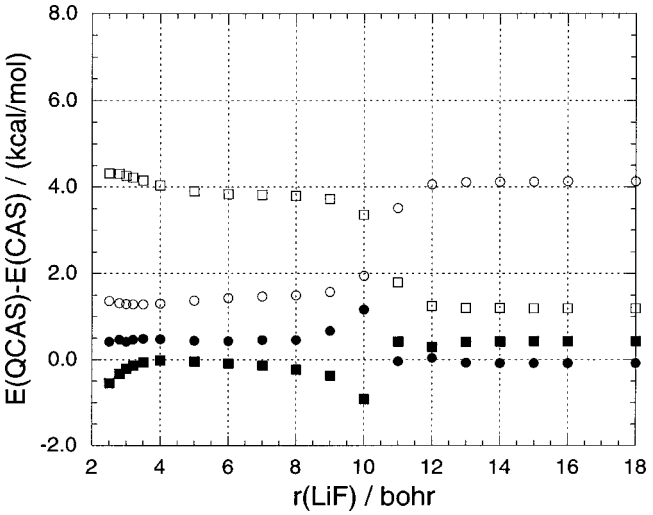

FIG. 3. The energy differences of the two lowest $^1\Sigma^+$ states of LiF between QCAS- and CAS-QDPT (the symbols ● and ■ are for the ground and excited states, respectively) and between QCAS- and CAS-SCF (○, □ for the ground and excited state, respectively).

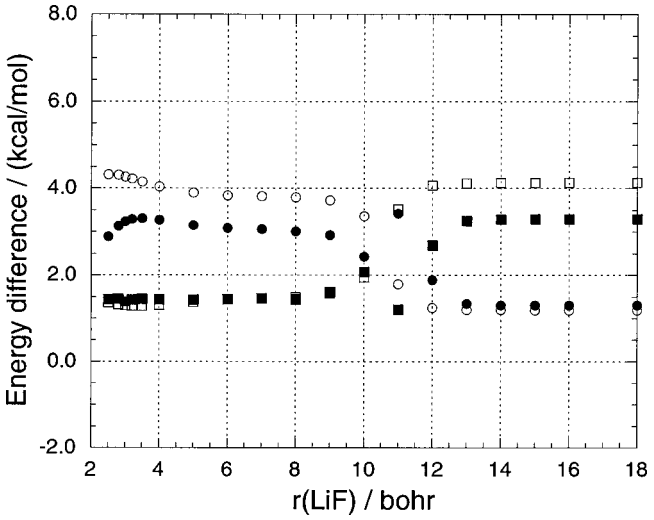

FIG. 4. The energy difference between QCAS-QDPT without the internal term contribution and CAS-QDPT (the symbols ● and ■ are for the ground and excited states, respectively) and between QCAS-SCF and CAS-SCF (○, □ for the ground and excited state, respectively).

B. Rydberg excitation energies of furan, C_4H_4O

Calculations were next carried out for the ground state and triplet and singlet Rydberg excited states of furan. An experimental geometry was used (the molecule is placed in the yz-plane).[32] The basis sets used for carbon and oxygen atoms are Dunning's correlation consistent polarized valence triple zeta (cc-pVTZ) set[33] except for the polarization functions, which were taken from those of cc-pVDZ.[33] The Rydberg functions ($2s2p2d$) were also placed on the charge center of the heavy atoms (C and O) of the molecule. The primitive Rydberg functions for C and O determined by Dunning and Hay[34] were weight-averaged and split into two with splitting factors of 1.9 and 0.75. The obtained exponents are 0.0471 (s), 0.0186 (s), 0.0426 (p), 0.0168 (p), 0.0285 (d), and 0.0113 (d). The cc-pVDZ set[33] was used for hydrogen atoms (no polarization on H).

We carried out the nine-state-averaged QCAS-SCF calculations for all $3s$, $3p$, and $3d$ Rydberg states. The active orbital set consists of five valence π and π^* orbitals and nine Rydberg orbitals. This orbital set was divided into two groups, five valence orbitals and nine Rydberg orbitals. For triplet Rydberg states, QCAS was constructed by distributing five electrons (three alpha and two beta electrons) to five valence orbitals and one alpha electron to nine Rydberg orbitals, QCAS$[(3\alpha 2\beta,5)\times(1\alpha,9)]$. For singlet Rydberg states, the active space was constructed from the QCASs that were made in a similar way to the triplet case, QCAS$[(3\alpha 2\beta,5)\times(1\beta,9)]$ and QCAS$[(2\alpha 3\beta,5)\times(1\alpha,9)]$. Since both of them are necessary for the active space to take into account proper spin-coupling, we use their direct sum, QCAS$[(3\alpha 2\beta,5)\times(1\beta,9)+(2\alpha 3\beta,5)\times(1\alpha,9)]$. These QCASs are applicable to the single excitations from a π valence orbital to a $3spd$ Rydberg orbital. The dimensions of the triplet and singlet QCASs are 900 and 1800, respectively. For the ground state, we used QCAS$[(6,5)\times(0,9)]$, which is equivalent to CAS(6,5).

Perturbation calculations were performed for the nine triplet and nine singlet $3spd$ Rydberg states and the ground state. The results are summarized in Table I as well as the experimental and our previous results.[35] We should note that the CAS-SCF calculations in the table were done for each individual symmetry including valence states. They are therefore different from the CAS-SCF using the *corresponding* CAS defined in Sec. II.

Singlet QCAS-SCF results are in good agreement with the CAS-SCF results (<0.1 eV) except for the $3p\,^1B_2$, $3d\,^1B_2$, and $3d\,^1A_1$ Rydberg states. For these states the CAS-SCF values are 0.21 ($3p\,^1B_2$), 0.18 ($3d\,^1B_2$), and 0.52 eV ($3d\,^1A_1$) higher than the QCAS-SCF values, since the CAS-SCF optimizations also included valence states of the same symmetry. On the other hand, the QCAS-QDPT results are very close to the CAS-QDPT results in all states. The average and maximum differences are only 0.03 eV and 0.11 eV, respectively. Moreover, the QCAS-QDPT excitation energies also reproduce the available experimental results well. The error is at most 0.11 eV.

Most triplet states are slightly lower than the corresponding singlet states (by 0.8 eV at maximum) in both the reference and QCAS-QDPT levels. Also in the triplet states, the QCAS-QDPT results are very close to the CAS-QDPT results, except for the $3d\,^3B_2$ state. The average and maximum differences are only 0.06 eV and 0.24 eV, respectively.

C. Transition state barrier height for the unimolecular dissociation reaction of formaldehyde $H_2CO \rightarrow H_2+CO$

The third example is the calculation of the transition state barrier height of the unimolecular dissociation reaction of formaldehyde, $H_2CO \rightarrow H_2+CO$. This reaction is Woodward–Hoffmann forbidden and therefore proceeds via the highly asymmetric transition structure as shown, for example, in Fig. 2 of the paper of Scuseria and Schaefer.[36] We examined in previous papers[37,10] the barrier height using a multireference perturbation method with the CAS-SCF reference function[37] and the QCAS-SCF method.[9] We now compare the QCAS-QDPT results with the CAS-QDPT results in the present article. Note that, since the reference is a single state, the QCAS-QDPT and CAS-QDPT are equivalent to QCAS-MRMP and CAS-MRMP, respectively.

The equilibrium and transition structures used are the same as in previous papers.[36,10,37] The complete active space we used for comparison is CAS(12,10), which is the full valence active space. We split the active orbitals into $\{CO(\sigma,\sigma^*)\}$, $\{CO(\pi,\pi^*)\}$, and $\{CH(\sigma,\sigma^*),CH(\sigma',\sigma'^*),O(lp,lp)\}$, where lp denotes a lone pair orbital, and then we distributed two, two, and eight electrons among the above groups, respectively, to construct QCAS$[(2,2)^2\times(8,6)]$. The dimension of the CAS is 44 100, while that of the QCAS is 3600.

The results with cc-pVTZ and cc-pVQZ[33] are shown in Table II. First let us compare the results at the reference function (QCAS- and CAS-SCF) level. Although differences in the energy itself between QCAS- and CAS-SCF are about 10 mhartree for both basis sets, the differences in the barrier height are 1.65 and 1.62 mhartree (1.0 and 1.0 kcal/mol) for

TABLE I. Rydberg excitation energies of furan (eV).

State	Singlet					Triplet			
	QCAS-SCF	QCAS-QDPT	CAS-SCF[a]	CAS-QDPT[a]	Exptl.[b]	QCAS-SCF	QCAS-QDPT	CAS-SCF	CAS-QDPT
$A_2(1a_2\rightarrow 3s)$	5.62	5.84	5.67	5.84	5.91	5.56	5.76	5.61	5.78
$B_1(1a_2\rightarrow 3pb_2)$	6.03	6.37	6.10	6.40	6.48	5.99	6.31	6.08	6.37
$B_2(1a_2\rightarrow 3pb_1)$	6.21	6.41	6.42	6.51	6.48	6.16	6.49	6.34	6.57
$A_2(1a_2\rightarrow 3pa_1)$	6.19	6.53	6.20	6.54	6.61	6.18	6.50	6.19	6.52
$A_2(1a_2\rightarrow 3da_1)$	6.61	6.96	6.64	6.98	⋯	6.55	6.86	6.58	6.88
$B_1(1a_2\rightarrow 3db_2)$	6.69	7.09	6.71	7.12	⋯	6.67	7.05	6.69	7.09
$A_2(1a_2\rightarrow 3da_1)$	6.77	7.19	6.77	7.19	⋯	6.75	7.15	6.75	7.16
$B_2(1a_2\rightarrow 3db_1)$	6.87	7.10	7.05	7.21	⋯	6.87	7.16	7.06	7.40
$A_1(1a_2\rightarrow 3da_2)$	6.82	7.30	7.34	7.29	7.28	6.77	7.23	7.11	7.28

[a]Reference 35.
[b]See references in Ref. 35.

cc-pVTZ and cc-pVQZ, respectively. The agreement of QCAS-SCF with CAS-SCF is very good.

Now let us compare the results at the MC-QDPT level. In total energy, there still remains a difference of about 8 mhartree between the results of QCAS- and CAS-QDPT, in contrast to the LiF case. In relative energy, for the barrier height the QCAS-QDPT results are very close to those of CAS-QDPT in both basis sets. The barrier height of QCAS-QDPT is 83.7 kcal/mol in both basis sets; the differences from those of CAS-QDPT are only 0.1 and 0.3 kcal/mol for cc-pVTZ and cc-pVQZ, respectively. Moreover, the barrier height is also close to the experimental value, 84.6 kcal/mol.[38] The error of 0.9 kcal/mol is within twice the experimental uncertainty 0.8 kcal/mol.

IV. CONCLUDING REMARKS

A second-order quasi-degenerate perturbation theory (QDPT) has been presented that is based on quasi-complete active space self-consistent field (QCAS-SCF) reference functions. The perturbation method shown here is an extension of a previously proposed QDPT with CAS-SCF reference functions and yet is a more efficient perturbation method that may employ a much smaller reference configuration space with the same number of active electrons and orbitals as in the CAS case.

A computational scheme using diagrammatic approach has been derived. The second-order QCAS-QDPT effective Hamiltonian is expressed by 25 external term and 9 internal term diagrams. The external term diagrams and five of the internal term diagrams are the same as those in CAS-QDPT and the conventional QDPT. The remaining four internal term diagrams are disconnected ones that do not appear in the CAS-QDPT case.

Since QCAS is a natural extension of CAS, computation of these diagrams can be done efficiently in a similar manner to CAS-QDPT. The summations for the orbital lines in the diagrams are done under the restriction such that the intermediate determinants/CSFs are outside the QCAS. In the QCAS reference case, this restriction is done only with orbital indices without referring to reference determinants/CSFs, whereas in the general reference case the restriction scheme depends also on the reference determinants/CSFs.

The method was tested on the potential energy curves of the LiF molecule, the Rydberg excitation energies of furan, and the transition state barrier height of the reaction, $H_2CO\rightarrow H_2+CO$. The results show that the present method yields very close results to the corresponding CAS-SCF reference MC-QDPT results and, moreover, it gives accurate estimates for the experimental values. Deviations from CAS-QDPT values in the energy were less than 0.1 eV on the average for the excitation energies of furan and less than 1 kcal for the barrier height of the reaction, $H_2CO\rightarrow H_2+CO$. The deviation from the experimental values was 0.11 eV at most for the excitation energies, and 1.2 kcal/mol, which is within the twice the experimental uncertainty, for the barrier height.

TABLE II. Transition state barrier height for the reaction $H_2CO\rightarrow H_2+CO$.

	Eq./hartree[a]	Tr./hartree[b]	ΔE/(kcal/mol)	Error/(kcal/mol)
cc-pVTZ				
CAS-SCF	−114.046 96	−113.913 81	83.6	−1.0
QCAS-SCF	−114.037 86	−113.903 06	84.6	0.0
CAS-QDPT[c]	−114.304 51	−114.171 34	83.6	−1.0
QCAS-QDPT[d]	−114.296 74	−114.163 38	83.7	−0.9
cc-pVQZ				
CAS-SCF	−114.056 24	−113.923 00	83.6	−1.0
QCAS-SCF	−114.047 12	−113.912 26	84.6	0.0
CAS-QDPT[c]	−114.330 57	−114.197 63	83.4	−1.2
QCAS-QDPT[d]	−114.323 16	−114.189 81	83.7	−0.9
Exptl. (classical)[e]			84.6±0.8	

[a]Equilibrium structure.
[b]Transition state structure.
[c]Equivalent to CAS-MRMP.
[d]Equivalent to QCAS-MRMP.
[e]Reference 38. Barrier height not including zero-point energy correction.

ACKNOWLEDGMENTS

The present research was supported in part by a Grant-in-Aid for Scientific Research on Priority Areas 'Molecular Physical Chemistry' from the Ministry of Education, Science, Sports and Culture of Japan. One of the authors (HN) acknowledges a Grant-in-Aid for Scientific Research from the Japan Society for the Promotion of Science. The MC-

SCF and perturbation calculations were carried out with a modified version of GAMESS (Ref. 7) and with MR2D (Ref. 6), respectively.

APPENDIX: DIAGRAM RULE IN THE SECOND-ORDER MC-QDPT

In the text, we used diagrams rather than the mathematical expression as often as we could in order to avoid lengthy equations. The effective Hamiltonian diagrams appearing in MC-QDPT to the second-order are identical to those in the conventional QDPT except for some disconnected ones. However, the rule for translating them into mathematical expression is somewhat different. In this Appendix, we describe it briefly for readers' convenience.

There are 25 diagrams for the external terms. Take one, for example:

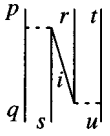

The diagram rule in conventional QDPT says that the contribution of this diagram to the second-order effective Hamiltonian is

$$(D_{\mathrm{ext}}^{\text{3-body}})_{pq,rs,tu}=-\sum_{i}^{\mathrm{core}}\frac{(pq|is)(ri|tu)}{\epsilon_i-\epsilon_r+\epsilon_u-\epsilon_t}E_{pq,rs,tu} \tag{A1}$$

in operator form and

$$(D_{\mathrm{ext}}^{\text{3-body}})_{AB}=-\sum_{pqrstu}^{\mathrm{act}}\sum_{i}^{\mathrm{core}}\frac{(pq|is)(ri|tu)}{\epsilon_i-\epsilon_r+\epsilon_u-\epsilon_t}\langle A|E_{pq,rs,tu}|B\rangle \tag{A2}$$

in matrix form. In MC-QDPT, the numerator and shift operator parts are common; however, the energy denominator is dependent of the determinant/CSF B and the reference state β:

$$D=\epsilon_i-\epsilon_r+\epsilon_u-\epsilon_t-E_B^{(0)}+E_\beta^{(0)}. \tag{A3}$$

Hence

$$(D_{\mathrm{ext}}^{\text{3-body}})_{AB}=-\sum_{pqrstu}^{\mathrm{act}}\sum_{i}^{\mathrm{core}}\frac{(pq|is)(ri|tu)}{\epsilon_i-\epsilon_r+\epsilon_u-\epsilon_t-E_B^{(0)}+E_\beta^{(0)}}\times\langle A|E_{pq,rs,tu}|B\rangle \tag{A4}$$

in matrix form. Multiplying Eq. (A4) by $C_A(\alpha)$ and $C_B(\beta)$ and taking summations over reference determinants/CSFs A and B, we obtain formulas for the second-order effective Hamiltonian for the reference states α and β from those for A and B:

$$(D_{\mathrm{ext}}^{\text{3-body}})_{\alpha\beta}=-\sum_{pqrstu}^{\mathrm{act}}\sum_{i}^{\mathrm{core}}\sum_{AB}^{\mathrm{Ref}}\frac{(pq|is)(ri|tu)}{\epsilon_i-\epsilon_r+\epsilon_u-\epsilon_t-E_B^{(0)}+E_\beta^{(0)}}\times C_A(\alpha)\langle A|E_{pq,rs,tu}|B\rangle C_B(\beta)$$

$$=-\sum_{pqrstu}^{\mathrm{act}}\sum_{i}^{\mathrm{core}}\sum_{B}^{\mathrm{Ref}}\frac{(pq|is)(ri|tu)}{\epsilon_i-\epsilon_r+\epsilon_u-\epsilon_t-E_B^{(0)}+E_\beta^{(0)}}\times\langle\alpha|E_{pq,rs,tu}|B\rangle C_B(\beta). \tag{A5}$$

The other external diagrams may be translated similarly.

For internal terms, all orbital lines in the product of the perturbation Hamiltonian are active orbital lines by definition: for example, the product of the two-body perturbation Hamiltonian,

$$V^{\text{2-body}}\cdot V^{\text{2-body}}=\sum_{pqrs}^{\mathrm{act}}\frac{1}{2}(pq|rs)E_{pq,rs}\times\sum_{tuvw}^{\mathrm{act}}\frac{1}{2}(tu|vw)E_{tu,vw}. \tag{A6}$$

The summation over active orbitals is restricted so that the intermediate determinants/CSFs should be outside the reference space, differing from the external term case. Thus all the diagrams derived from the product including disconnected one survive:

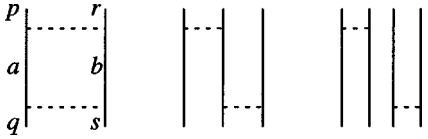

The three-body connected and four-body disconnected diagram have been already given in Eqs. (10) and (11) in the text, respectively. The two-body connected diagram represents the following mathematical expression:

$$(D_{\mathrm{int}}^{\text{2-body}})_{\alpha\beta}=\frac{1}{2}\sum_{pqrstu}^{\mathrm{act}}\sum_{ab}^{\mathrm{act}}\sum_{AB}^{\mathrm{Ref}}\frac{(pa|rb)(aq|bs)}{\epsilon_q-\epsilon_a+\epsilon_s-\epsilon_b-E_B^{(0)}+E_\beta^{(0)}}\times\langle\alpha|E_{pq,rs}|B\rangle C_B(\beta). \tag{A7}$$

The other internal terms, derived from the product including one-body perturbation, may be derived similarly.

The rules for obtaining mathematical expressions for the second-order effective Hamiltonian diagram are summarized as follows:

(a) The product of the CI coefficient $C_B(\beta)$ and the coupling coefficient $\langle\alpha|E_{pq,\cdots,rs}|B\rangle$ between the state α and determinant/CSF B for free particle lines. The index pair $(pq),\cdots,(rs)$ in the shift operator $E_{pq,\cdots,rs}$ originate from the lines connected through a vertex (or vertices).

(b) A molecular integral [a two-electron integral $(ij|kl)$ or a modified one-electron integral v_{pq}] for each interaction line, where the modified one-electron integral ν_{pq} is defined by

$$v_{pq}=h_{pq}+\sum_{i}^{\mathrm{core}}[2(pq|ii)-(pi|iq)]. \tag{A8}$$

An energy denominator for the lower interaction line,

$$D=\sum(\epsilon_{\text{annihilation}}-\epsilon_{\text{creation}})-E_B^{(0)}+E_\beta^{(0)}, \tag{A9}$$

where $\epsilon_{\text{annihilation}}$ and $\epsilon_{\text{creation}}$ represent energies of orbitals corresponding to annihilation and creation operators, respectively. The summation is taken for all the annihilation and creation operator labels associated with the lower interaction line.

A factor of $(1/2)^{n+l}$, where n is the number of equivalent diagrams and l is the number of loops.

A factor of $(-1)^{h+l}$, where h is the number of internal hole (core) lines.

Summation for all the orbital lines. Here, for the internal term diagrams, the summation for active orbitals is restricted so that the intermediate determinants/CSFs should be outside the reference space.

Summation for determinants/CSFs B.

Factors (a) and (c) and summation (g) are different from the usual Goldstone diagram rule. We should note that these rules are specialized to the second-order effective Hamiltonian and do not apply for higher order.

[1] K. Hirao, Chem. Phys. Lett. **190**, 374 (1992).
[2] K. Hirao, Chem. Phys. Lett. **196**, 397 (1992).
[3] K. Hirao, Int. J. Quantum Chem., Symp. **26**, 517 (1992).
[4] H. Nakano, J. Chem. Phys. **99**, 7983 (1993).
[5] H. Nakano, Chem. Phys. Lett. **207**, 372 (1993).
[6] MR2D Ver. 2, H. Nakano, University of Tokyo, 1995.
[7] M. W. Schmidt, K. K. Baldridge, J. A. Boatz *et al.*, J. Comput. Chem. **14**, 1347 (1993).
[8] M. Dupuis, S. Chin, and A. Marquez, in *Relativistic and Electron Correlation Effects in Molecules and Clusters*, NATO ASI Series, edited by G. L. Malli (Plenum, New York, 1992), p. 315.
[9] Exactly, CSF selection according to the magnitude of the CAS-CI coefficients is now available in both GAMESS and HONDO. The contribution from unselected CSFs is taken into account perturbatively.
[10] H. Nakano and K. Hirao, Chem. Phys. Lett. **317**, 90 (2000).
[11] G. Hose and U. Kaldor, J. Phys. B **12**, 3827 (1979).
[12] A. Haque and D. Mukherjee, Pramana **23**, 651 (1984).
[13] B. Jeziorski and H. J. Monkhorst, Phys. Rev. A **24**, 1668 (1981).
[14] D. Mukherjee, Proc. Indian Acad. Sci. Chem. Sci. **96**, 145 (1986).
[15] D. Mukherjee, Chem. Phys. Lett. **125**, 207 (1986).
[16] W. Kutzelnigg, J. Chem. Phys. **77**, 3081 (1982).
[17] W. Kutzelnigg and S. Koch, J. Chem. Phys. **79**, 4315 (1983).
[18] W. Kutzelnigg, D. Mukherjee, and S. Koch, J. Chem. Phys. **87**, 5902 (1987).
[19] D. Mukherjee, W. Kutzelnigg, and S. Koch, J. Chem. Phys. **87**, 5911 (1987).
[20] P. Celani and H.-J. Werner, J. Chem. Phys. **112**, 5546 (2000).
[21] S. Grimme and M. Waletzke, Phys. Chem. Chem. Phys. **2**, 2075 (2000).
[22] K. Andersson, P.-Å. Malmqvist, B. O. Roos, A. J. Sadley, and K. Wolinski, J. Phys. Chem. **94**, 5483 (1990).
[23] K. Andersson, P.-Å. Malmqvist, and B. O. Roos, J. Chem. Phys. **96**, 1218 (1992).
[24] R. B. Murphy and R. P. Messmer, Chem. Phys. Lett. **183**, 443 (1991).
[25] R. B. Murphy and R. P. Messmer, J. Chem. Phys. **97**, 4170 (1992).
[26] R. Cimiraglia, J. Chem. Phys. **83**, 1746 (1985).
[27] B. Huron, J.-P. Malrieu, and P. Rancurel, J. Chem. Phys. **58**, 5745 (1973).
[28] The definition of QCAS in the present paper is somewhat different from that of Ref. 18.
[29] I. Lindgren and J. Morrison, *Atomic Many-Body Theory*, 2nd ed. (Springer-Verlag, New York, 1982).
[30] J.-P. Malrieu, J.-L. Heully, and A. Zaitsevskii, Theor. Chim. Acta **90**, 167 (1995).
[31] R. Krishnan, J. S. Binkley, R. Seeger, and J. A. Pople, J. Chem. Phys. **72**, 650 (1980).
[32] B. Bak, L. Hansen, and J. Rastrup-Andersen, Discuss. Faraday Soc. **19**, 30 (1955).
[33] T. H. Dunning, Jr., J. Chem. Phys. **90**, 1007 (1989).
[34] T. H. Dunning, Jr. and P. J. Hay, in *Methods of Electronic Structure Theory*, edited by H. F. Schaefer III (Plenum, New York, 1977), Vol. 3, p. 1.
[35] H. Nakano, T. Tsuneda, T. Hashimoto, and K. Hirao, J. Chem. Phys. **104**, 2312 (1996).
[36] G. E. Scuseria and H. F. Schaefer III, J. Chem. Phys. **90**, 3629 (1989).
[37] H. Nakano, K. Nakayama, K. Hirao, and M. Dupuis, J. Chem. Phys. **106**, 4912 (1997).
[38] W. F. Polik, D. R. Guyer, and C. B. Moore, J. Chem. Phys. **92**, 3453 (1990).